26 May 2010, 4:45 pm - 6:45 pm

Analysis of Tunnel Behaviour Under Seismic Loads by Means of Simple and Advanced Numerical Approaches

Daniela Boldini
University of Bologna, Italy

Angelo Amorosi
Technical University of Bari, Italy

Fabrizio Palmisano
Technical University of Bari, Italy


Fifth International Conference on
Recent Advances in Geotechnical Earthquake Engineering and Soil Dynamics
and Symposium in Honor of Professor I.M. Idriss
May 24-29, 2010 • San Diego, California

ANALYSIS OF TUNNEL BEHAVIOUR UNDER SEISMIC LOADS BY MEANS OF SIMPLE AND ADVANCED NUMERICAL APPROACHES

Daniela Boldini
University of Bologna
Bologna, Italy

Angelo Amorosi
Technical University of Bari
Bari, Italy

Fabrizio Palmisano
Technical University of Bari
Taranto, Italy

ABSTRACT

In this paper different approaches aimed at investigating the dynamic behaviour of circular tunnels in the transverse direction are presented. The analysed cases refer to a shallow tunnel built in an ideal soft clayey deposit. The adopted approaches include one-dimensional (1D) numerical analyses performed modelling the soil as a single phase visco-elastic non-linear medium, the results of which are then used to evaluate the input data for selected analytical solutions proposed in the literature (uncoupled approach), and 2D fully coupled Finite Element simulations adopting visco-elastic and visco-elasto-plastic constitutive assumptions for the soil and the lining (coupled approach). The results are proposed in terms of increments of seismic-induced loads in the transverse direction of the tunnel lining. The different constitutive hypotheses adopted in the coupled numerical approach prove to play a significant role on the results. In particular, the plasticity-based analyses indicate that a seismic event can produce a substantial modification of the loads acting in the lining, leading to permanent increments of both hoop force and bending moment.

INTRODUCTION

The dynamic response of tunnels to seismic actions can be assessed by means of uncoupled or coupled approaches, depending on whether the evaluation of the seismic wave propagation and of the corresponding actions on the structure is undertaken in two separated steps or in one single analysis, respectively.

In this work, the uncoupled approach consisting in 1D visco-elastic analyses performed using the equivalent linear code EERA (Bardet *et al.* 2000), is aimed at establishing the role of stiffness and damping non-linearity on the free-field site response. The results of the analyses at the tunnel depth are then used to evaluate the input data for selected analytical solutions proposed in the literature to predict the transverse response of the structure for both full-slip and no-slip conditions (e.g. Wang 1993).

To overcome some of the limitations of the approach described above, a fully coupled Finite Element (FE) analysis is here adopted simulating in the time domain the soil-structure dynamic interaction during the seismic event. This latter is in this case realistically described by an accelerogram, while for the soil an effective stress formulation is adopted.

The constitutive assumption for the soil is a key element of this class of analyses. A first analysis (analysis *VE_ve*) is carried out assuming a linear visco-elastic model for both the soil and the lining. The viscous damping is introduced by means of the Rayleigh formulation. In this context, it emerges that the appropriate selection of the elastic and viscous soil parameters profile with depth deserves particular attention, as the results are strongly influenced by it. In this work a strategy to calibrate the parameters for the visco-elastic soil model is proposed based on the free field soil response results obtained in the context of the uncoupled approach.

A second set of analyses is carried out assuming a visco-elasto-plastic assumption for the soil. Despite the relatively simple formulation adopted, the analyses highlight a number of peculiar aspects that significantly differ from the linear ones: re-distribution of the soil stress regime around the tunnel, leading to different distribution of the hoop force and bending moments in the tunnel lining, both during and after the earthquake. In a first attempt to focus more specifically on the structural response of the tunnel lining, two possible options are adopted for its constitutive description, namely

visco-elastic (analysis *VEP_ve*) and visco-elasto-plastic (analysis *VEP_vep*), leading to different temporary and permanent load regimes acting on the structure.
Concerning this latter finding, it is worth remarking that modern seismic structural design includes, in general, two different approaches: design for strength or design for ductility and energy dissipation. Although technically feasible, designing a structure to respond elastically to seismic actions (strength approach) is economically prohibitive in most cases. It could also be unnecessary as an earthquake is a dynamic action representing, for a structure, an energy input and a demand to tolerate certain displacements and deformations but not a demand to withstand specific forces.
This is the reason why the most widespread design approach is the one that allows the structure to develop significant inelastic deformation under the seismic action, retaining a residual load bearing capacity after the seismic events. It is worth noting that this approach is significantly different from that adopted for other loading conditions. While for static actions no damage is allowed under design loads, it is tolerated during the earthquake when adopting a dissipative approach in the design.
In this context, tunnels are very peculiar structures. In fact, on one hand, considering the consequences of their collapse for human life or their importance for public safety and civil protection in the immediate post-earthquake period, they should be designed following a strength approach. Nonetheless, in a different prospective, considering the necessity to make them tolerate large displacements and deformations, a ductility approach seems to be the only feasible. Therefore, a successful tunnel design is the one that is able to achieve a satisfactory balance between strength and ductility.

OUTLINE OF THE IDEALISED PROBLEM

A 60-m thick ideal deposit of soft clay is assumed as the reference soil profile. The physical properties and mechanical parameters are reported in Table 1. The water table is assumed at the ground surface.
The assumed profile of the small-strain shear stiffness G0 with depth (Fig. 1) was calculated adopting the relationship proposed by Viggiani (1992):

$$\frac{G_0}{p_r} = S \cdot \left(\frac{p'}{p_r} \right)^n \cdot R^m \qquad (1)$$

where p_r is a reference pressure taken equal to 1 kPa, p' is the mean pressure, S, n and m are parameters depending on the plasticity index I_P and R is the overconsolidation ratio in terms of mean effective stress. The values of S, n and m are also summarised in Table 1.
For sake of simplicity, the small-strain damping ratio D_0 was considered constant with depth.

Table 1. Physical and mechanical parameters of the soft clay deposit.

Parameters:	
Plasticity index I_P (%)	44
Unit weight of volume γ (kN/m^3)	17
Coefficient at rest K_0	0.60
Overconsolidation ratio in terms of mean effective stress R	1.5
Small-strain shear stiffness G_0 (MPa)	variable with depth (Figure 1)
Small-strain damping ratio D_0 (%)	1.0
Poisson's ratio v'	0.25
Cohesion c' (kPa)	0
Friction angle φ' (°)	24
Parameter of Eq. (1) S	600
Parameter of Eq. (1) n	0.820
Parameter of Eq. (1) m	0.360

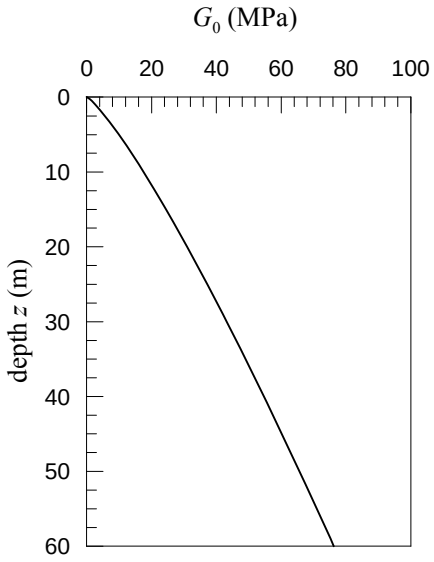

Fig. 1. Profile of the small-strain shear stiffness G_0.

A circular tunnel, located at 15 m depth and with a 10.10 m diameter, is selected as the reference underground structure for the present case study. The lining is assumed to be composed by 0.50 m thick reinforced concrete ring, characterised by a characteristic compressive cubic strength of the concrete R_{ck} = 45 MPa and by the following linear visco-elastic parameters: Young's modulus E_l = 38 GPa, Poisson's ratio v_l = 0.25, damping ratio D_l = 5%.
In the present study the acceleration time history recorded at Kalamata (Greece) during the 13.XI.1986 earthquake was considered. The original seismic signal is characterised by a duration of 29.74 s and by a maximum acceleration of 0.24 g.
The input signal was scaled to 0.35 g and was filtered to

prevent frequency levels higher than 7 Hz. This latter frequency was selected consistently with the element dimension adopted in the FE discretisation. A diagram of the selected horizontal component of the acceleration time history after manipulation is given in Fig. 2 while the corresponding Fourier spectrum is shown in Fig. 3.
The input seismic signal was considered as applied at the rock outcropping of the deposit. The corresponding bedrock motion was then calculated by performing an equivalent-linear deconvolution with the code EERA.

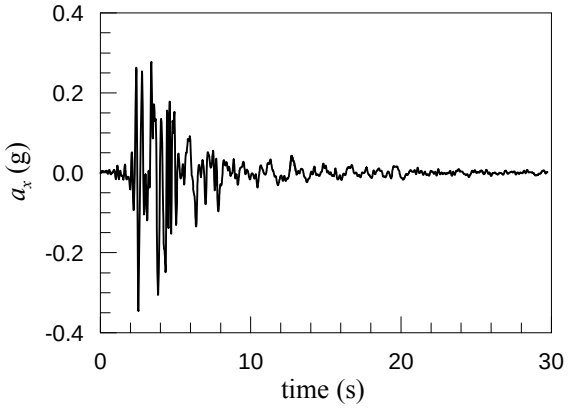

Fig. 2. Modified acceleration time history scaled at 0.35 g.

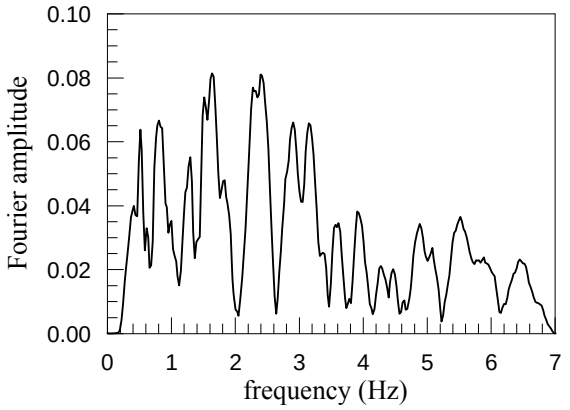

Fig. 3. Frequency-filtered Fourier spectrum.

1D EQUIVALENT-LINEAR VISCO-ELASTIC GROUND RESPONSE ANALYSIS

The 1D ground response analyses were performed by the code EERA (Bardet *et al.* 2000). The code is based on the assumption of equivalent-linear visco-elastic soil behaviour.
Modulus reduction curve G/G_0 and variation of damping ratio D with shear strain level γ were defined according to typical results reported in the literature (Vusetic and Dobry 1991) as a function of I_P (Fig. 4).
A total number of 31 layers were assumed to discretise the profiles of stiffness and damping ratio with depth: 1 uppermost layer of 0.5 m thickness, followed by 10 of 1 m, 15 of 3 m, 4 of 4 m and 1 base layer of 3.5 m. In the iterative procedure the ratio of effective and maximum shear strain is assumed equal to 0.5.
Fig. 5 shows the results of the analysis in terms of maximum shear strain γ_{max}, normalised shear stiffness G/G_0, damping ratio D and maximum acceleration a_{max}. Values of γ_{max} (equal to 0.625 %) and G obtained at the depth of 15 m, i.e. at the tunnel depth, were subsequently used to evaluate the increments in the hoop force and bending moment in the tunnel lining during the earthquake, according to selected analytical solutions discussed in the next paragraph.

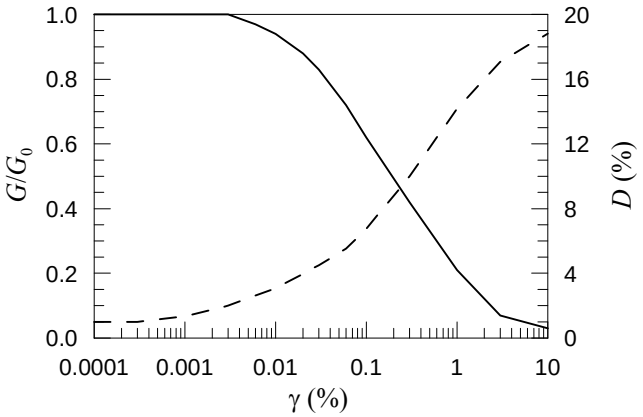

Fig. 4. Modulus reduction curve G/G_O and variation of damping ratio D with shear strain γ.

ANALYTICAL SOLUTIONS

Here, the closed-form solutions summarised in Wang (1993) to predict the traverse response of the tunnel are adopted, according to what suggested by Hashash *et al*. (2005). These solutions take explicitly into account the soil-structure interaction effect under both *no-slip* and *full-slip* conditions. They are based on the following assumptions:

- the ground is an infinite, elastic, homogeneous and isotropic medium;
- the tunnel and the lining are circular and the lining thickness is small in comparison to the tunnel diameter.

Seismic actions are considered as external static forces acting on the tunnel lining, induced by the ground distortion related to a vertically propagating shear wave. The resulting ovalisation of the tunnel lining is assumed to occur under plane strain conditions.
According to Wang (1993), the flexibility ratio F is the most important parameter to quantify the ability of the lining to resist against the distortion imposed by the ground:

$$F = \frac{E_u\left(1-\nu_l^2\right)r^3}{6E_l I\left(1+\nu_u\right)} \qquad (2)$$

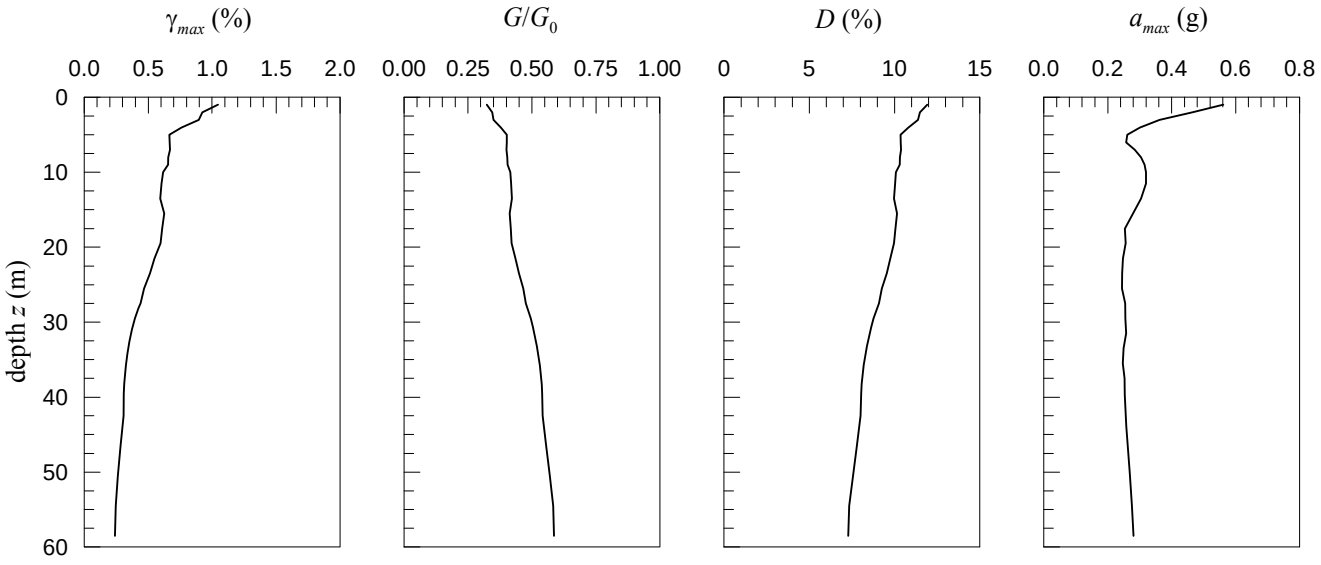

Fig. 5. Results of the 1D ground response analysis performed with EERA.

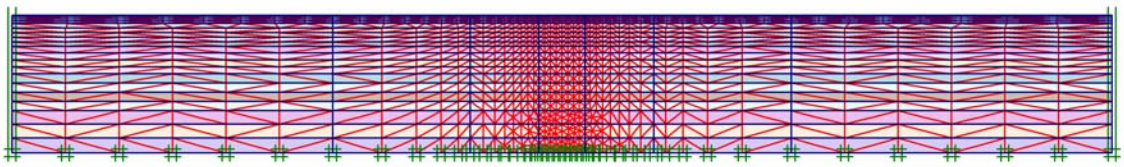

Fig. 6. Mesh employed in the FEM analyses.

where E_u and ν_u indicate the mobilised soil Young's modulus (evaluated with reference to the previously calculated mobilised shear modulus G) and the Poisson's ratio (assumed equal to 0.5) in undrained conditions, respectively. t and I the thickness and the moment of inertia of the tunnel lining, respectively.

For the investigated case F is equal to 1.0, i.e. the flexural stiffness of the lining corresponds to the flexural stiffness of the excavated soil material inside the tunnel cavity ("non-perforated" condition). In this case no relevant slippage between the soil and the tunnel lining is expected.

Table 2 summarises the increments in the hoop force and bending moment of the tunnel lining computed for both *full-slip* and *no-slip* conditions. Increments in the hoop force, as expected, are significantly higher in the *no-slip* case. Increments in the bending moment coincide, irrespectively of the different slippage conditions assumed in the analyses.

2D FE NUMERICAL MODELLING

The coupled numerical analyses were performed with the Finite Element code PLAXIS 2D (2003), a two-dimensional (plane strain and axi-symmetric) code that implements the coupled Biot dynamic equations (Biot 1941) adopting the so called *u-p* simplification (where *u* is the skeleton displacement and *p* the pore pressure), assuming as negligible the fluid acceleration relative to the solid skeleton.

The code adopts the Generalised Newmark method (Katona and Zienkiewicz 1985) for the time integration under dynamic conditions. In this case the following standard values of the Newmark's constants were selected in all the analyses illustrated in this paper: $\alpha_N = 0.3025$ and $\beta_N = 0.6000$. Those values ensure that the algorithm is unconditionally stable, while being dissipative only for the high-frequency modes.

In the dynamic solution the code allows to introduce frequency dependent viscous damping by means of the Rayleigh formulation, the damping matrix being defined as follows:

Table 2. Increments of hoop force and bending moment according to Wang (1993).

full-slip conditions		*no-slip* conditions	
$\Delta N_{max,min}$ (kN/m)	$\Delta M_{max,min}$ (kNm/m)	$\Delta N_{max,min}$ (kN/m)	$\Delta M_{max,min}$ (kNm/m)
±159	**±802**	**±473**	**±802**

In the dynamic solution the code allows to introduce frequency dependent viscous damping by means of the Rayleigh formulation, the damping matrix being defined as follows:

$$[\mathrm{C}] = \alpha_R [\mathrm{M}] + \beta_R [\mathrm{K}] \tag{3}$$

where $[\mathrm{M}]$ and $[\mathrm{K}]$ are the mass and the stiffness matrix of the system, respectively. The coefficients α_R and β_R are obtained considering the following relationship with the damping ratio D (e.g. Clough and Penzien 1993):

$$\begin{Bmatrix} \alpha_R \\ \beta_R \end{Bmatrix} = \frac{2D}{\omega_n + \omega_m} \begin{Bmatrix} \omega_n \omega_m \\ 1 \end{Bmatrix} \tag{4}$$

where ω_n e ω_m are the angular frequencies related to the frequency interval $f_n \div f_m$ in which the viscous damping is equal to or lower than D.

The boundary conditions adopted for the static stages of the analyses were the standard ones: nodes at the bottom of the mesh were fixed in both vertical and horizontal directions, while those along the lateral sides were only fixed in the horizontal direction. In the dynamic analyses the bottom of the mesh was assumed to be rigid and the lateral sides were characterised by the viscous boundaries proposed by Lysmer and Kuhlmeyer (1969), with parameters a= 1.0 and b = 0.25.

In order to perform a comparative analysis with the EERA results, a linear visco-elastic constitutive model for the soil was first selected in the dynamic stage of the analyses, coupling a linear isotropic elastic model and the Rayleigh viscous formulation. Plasticity was then added, leading to a non-associated visco-elasto-plastic constitutive assumption characterised by a Mohr-Coulomb yield criterion and a null dilatancy angle.

The structural elements adopted to simulate the tunnel lining were firstly assumed to be linear visco-elastic plates, formulated according to the Mindlin theory (e.g. Bathe 1982). Impervious interface elements were also introduced to model the interaction between the lining and the soil, according to the formulation summarised in the manual of the code. In particular, the interface was characterised by values of the shear strength parameters equal to those of the surrounding soil: such an assumption can be considered as corresponding to the no-slip condition of the Wang's solutions.

Plasticity was then added to the structure assuming a simplified diamond-shape interaction diagram between bending moment and axial action. In this case the following parameters were used: effective depth of the cross section d = 0.43 m, characteristic yield strength of the reinforcement f_{yk} = 450 MPa. According to Eurocode 8 (CEN 2004b), mean values of material strength were assumed. In particular: compressive strength of concrete f_{cm} = 43 MPa (CEN 2004a) and yield strength of reinforcement f_{ym} = 517.5 MPa (Fardis et *al.* 2005). Two different reinforcement ratio conditions were analysed. In the first case (*VEP_vep_1*) the reinforcement ratio for longitudinal tensile and compressive reinforcement was assumed equal to 0.3% while in the second case (*VEP_vep_2*) a value of 0.15% was used.

According to CEN 2004a a parabola-rectangle diagram for concrete under compression was assumed with strain at the maximum strength ε_{c2} = 0.2% and ultimate strain ε_{cu2} = 0.35%. For the reinforcement a bilinear elastic perfectly plastic stress-strain diagram was used with yield strain ε_{ym} = 0.26% and extreme strain ε_{uk} = 7.5% .

From these assumptions the following characteristic points (M_p = maximum bending moment for pure flexure; N_p = maximum compressive axial force in absence of bending moment) were calculated: $|M_p|$ = 327 kNm/m and N_p = -23053 kN/m in *VEP_vep_1*, $|M_p|$ = 165 kNm/m and N_p = -22276 kN/m in *VEP_vep_2*.

It is worth nothing that since the code Plaxis uses only symmetrical diamond-shape interaction diagrams, the maximum tensile axial force was assumed equal to the absolute value of the maximum compressive one. Even though this assumption appears as unrealistic for a r.c. structure, it did not affect the results of the analyses described below, as the axial force is always characterised by compressive states.

The mesh employed in the present study is reported in Figure 6: it is characterised by a width equal to 8 times its height, in order to minimise the influence of boundary conditions on the computed results. The domain was discretised in a total number of 2431 15-node plane strain triangular elements.

In the central part of the mesh, where the tunnel is located, the characteristic dimension of the elements h always satisfies the condition:

$$h \le h_{\max} = V_S / (6 \div 7) f_{\max} \tag{5}$$

where V_S is the shear wave velocity and f_{max} is the maximum frequency of the seismic signal.

The domain was partitioned into 20 horizontal layers to account for variable stiffness and damping parameters with depth.

A detail of the mesh around the tunnel is shown in Fig. 7.

All the analyses were carried out performing a set of initial static stages, to simulate the tunnel excavation, the installation of the lining and the subsequent consolidation stage, followed by the dynamic stage, during which the seismic signal was applied at the bottom of the mesh, and a final static post-seismic consolidation stage.

In particular, the simulation of the tunnel excavation was performed in undrained conditions by imposing a volumetric contraction of the tunnel section corresponding to a volume loss of 0.4 %. This value was selected as representative of a satisfactory performance of the tunnel excavation stage for a shallow tunnel in clayey material. The following installation of the tunnel lining was also carried out under undrained conditions, while in the subsequent consolidation stage the previously cumulated excess pore water pressures were allowed to dissipate, leading to the pre-seismic reference state

of the system. The dynamic stage was then carried out under undrained conditions, adopting a time step equal to 0.03 s, corresponding to that of the seismic signal input data. A post-seismic consolidation analysis was finally performed, to evaluate the long term effects of the seismic event on the tunnel section.
The elastic soil shear stiffness moduli G assumed in the static stages of the analyses were selected scaling down the corresponding initial values G_0 according to the normalised modulus reduction curves shown in Fig. 4, assuming an average mobilised shear strain level equal to 0.1%.
All the static stages of the analyses were also characterised by the assumption of elasto-plastic behaviour of the soil, irrespectively of the hypotheses holding for the dynamic stages. This was aimed at reproducing the same pre-seismic conditions for all the dynamic analyses.

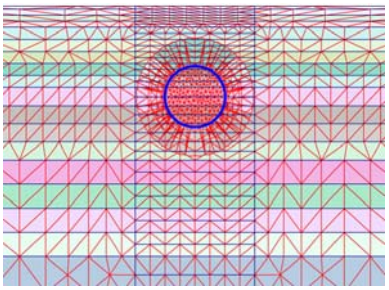

Fig. 7. Detail of the mesh around the tunnel section.

CALIBRATION OF THE VISCO-ELASTIC PARAMETERS AND FREE-FIELD FE GROUND RESPONSE ANALYSES

The analysis of soil dynamic boundary value problems is often based on constitutive assumptions characterised by visco-elastic hypotheses for the reversible response. In this context it is a well-established fact that the solution depends on the assumed profile of the stiffness and damping parameters with depth (e.g. Kramer 1996). Thus, when adopting linear visco-elastic assumptions the parameter calibration might not be trivial (e.g. Woodward and Griffiths 1996), due to the well-known dependency of both stiffness and damping on the strain level.
In this paper, a recently developed calibration procedure of the visco-elastic parameters to be assumed in dynamic FE analyses is proposed (Amorosi and Boldini 2009). G and D profiles are set in such a way to match the corresponding profiles resulting from the free-field EERA analysis. For each layer a single value of G and D is selected, together with the corresponding Rayleigh coefficients α_R and β_R. These two coefficients are chosen according to Equation (4), for the frequency interval $f_n \div f_m$ characterised by the highest energy content predicted by EERA at different depths of the soil deposit.
Fourier spectra computed with EERA at different depths are reported in Fig. 8 together with the frequency interval selected for the definition of the Rayleigh coefficients according to Equation (4): in this case the highest energy content is observed between 0.4 and 2.6 Hz.
A preliminary comparison between the EERA and PLAXIS predictions at the tunnel depth is provided to check the consistency between the 1D and 2D approaches. In this case the 2D FE model does not incorporate the tunnel and, as such, the PLAXIS results can be directly compared to that of the corresponding 1D free-field analysis performed with EERA. A comparison between the acceleration time histories and the corresponding Fourier amplitude computed at $z = 15$ m with EERA and with the visco-elastic PLAXIS analysis is illustrated in Fig. 9. A good agreement is obtained, demonstrating the effectiveness of the proposed calibration strategy.

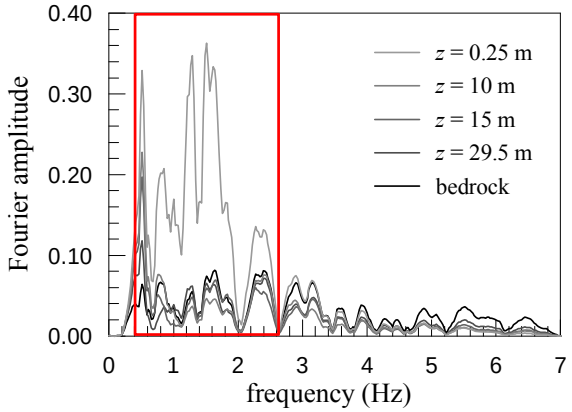

Fig. 8. Fourier spectra computer by EERA at different depths and high-energy frequency interval.

FE NUMERICAL ANALYSES OF THE TUNNEL

Analysis *VE_ve*

The distribution of the predicted hoop force N and bending moment M prior to and after the earthquake, as well as their minimum and maximum envelopes during the seismic event, are shown in Fig. 10a,b for the analysis *VE_ve*. The results are reported as a function of the angle θ, also shown in Fig. 10, and defined positive in counter-wise direction.
Results indicate a good agreement between the visco-elastic FE solution, characterised by maximum increments, evaluated with respect to the static conditions, of hoop force $|\Delta N|_{max}$ = 426 kN/m and bending moment $|\Delta M|_{max}$ = 713 kNm/m, and the corresponding increments predicted by the Wang's solutions for the no-slip case (Table 2). These latter are only slightly larger than the numerical results both in terms of hoop force (+ 11 %) and bending moment (+ 13 %). It is worth remarking that the two solutions compared above are based on substantially different approaches: the analytical results rely on a quasi-static analysis of the problem, while the dynamic FE solution includes more realistic features like the time

dependent kinematic soil-structure interaction. Nonetheless, the results compare nicely in the visco-elastic case.

Analysis *VEP_ve*

Adding soil plasticity to the FE analysis (Fig. 10c,d) significantly modifies the stress distribution in the lining both qualitatively and quantitatively. In fact, the behaviour during the earthquake is characterised by reduced loads in the tunnel lining as compared to the visco-elastic case, especially in terms of bending moment: uppermost increments with respect to the static conditions are in this case equal to $|\Delta N|_{max}$ = 356 kN/m and $|\Delta M|_{max}$ = 499 kNm/m. This pattern is consistent with what observed by Shahrour and Khoshnoudian (2003) for plasticity based dynamic analyses of shallow tunnels in soft soils. More important, permanent increments of hoop force and bending moment are predicted at the end of the seismic event, as a consequence of the irreversible deformation cumulated by the soil during the earthquake. In particular, the permanent increment of hoop force with respect to the initial static conditions, entirely in compression, is characterized by a maximum value of ΔN = - 313 kN/m at the tunnel crown, while that of bending moment ΔM varies between - 340 kNm/m and + 349 kNm/m.

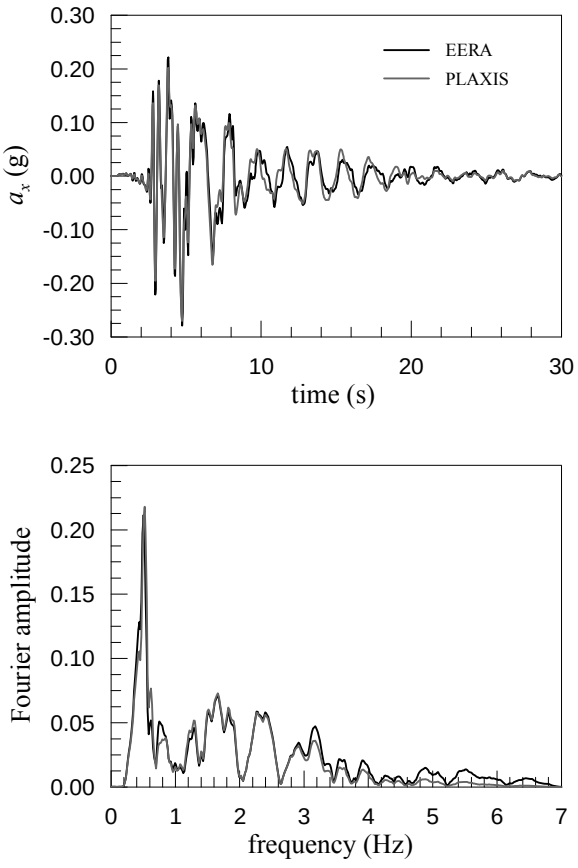

Fig. 9. Comparison between EERA and PLAXIS free-field soil response analyses at 15 m depth.

Fig. 11 illustrates the evolution of the hoop force and bending moment during the earthquake in the analyses *VE_ve* and *VEP_ve* for $\theta = 135°$. The plasticity based analysis shows a noticeable accumulation of permanent loads starting from $t \cong 2.5$ seconds, approximately corresponding to the peak value of the accelerogram at the tunnel depth.

The results of the *VEP_ve* analysis indicate that the irreversible soil behaviour significantly modifies the tunnel loads both during the earthquake and, more importantly, after it.

In fact, albeit the simple perfectly plastic constitutive assumption adopted, a considerable amount of plastic strain cumulate in the soil during the dynamic analyses, leading to a corresponding permanent modification of the effective stress distribution around the tunnel lining.

All the plasticity-based analyses proposed in this work are characterised by a post-seismic consolidation stage, aimed at evaluating the effects on the tunnel lining of the dissipation of the excess pore water pressures induced during the shaking. It results that these effects are negligible in the cases under study, given the low excess pore water pressures predicted by the relatively simple constitutive model adopted for the clayey material (Fig. 12).

Analyses *VEP_vep_1* and *VEP_vep_2*

In order to investigate the influence on the overall behaviour of the mechanical characteristics of the lining, two FE analyses including the visco-elasto-plastic constitutive assumption for the soil as well as a simplified visco-elasto-plastic model for the tunnel lining were performed.

The assumption of elasto-plastic response of the lining mainly influences the flexural behaviour of the tunnel itself. The distribution of the predicted hoop force N and bending moment M prior to and after the earthquake, as well as their minimum and maximum envelopes during the seismic event, are shown in Fig. 10e,f,g,h. Figures 10f and 10h clearly show that, due to plasticity, a reduction of the maximum bending moment during and after the earthquake is observed.

It is worth noting that the simple choice of a linear (diamond-shape) interaction diagram between bending moment and axial action induces negligible errors, due to the low values of the hoop force resulting for the problem under study.

Having assumed a visco-elasto-plastic model for the tunnel, a curvature check is needed. Since Plaxis does not provide any information on the curvature, pushover analyses were performed, adopting the code Midas/Gen (2007).

In particular, the displacement obtained for each step of *VEP_vep_1* and *VEP_vep_2* were used to detect the conditions of maximum overall deformation. These latter were defined with reference to the maximum elongation of either the vertical or the horizontal diameter of the tunnel. In both analyses the maximum deformation was observed at the end of the earthquake (t = 30s), due to the progressive accumulation of irreversible strain with increasing number of cycles. Finally, these elongations were adopted as target displacements in the pushover analysis. Fig.13a,b shows the

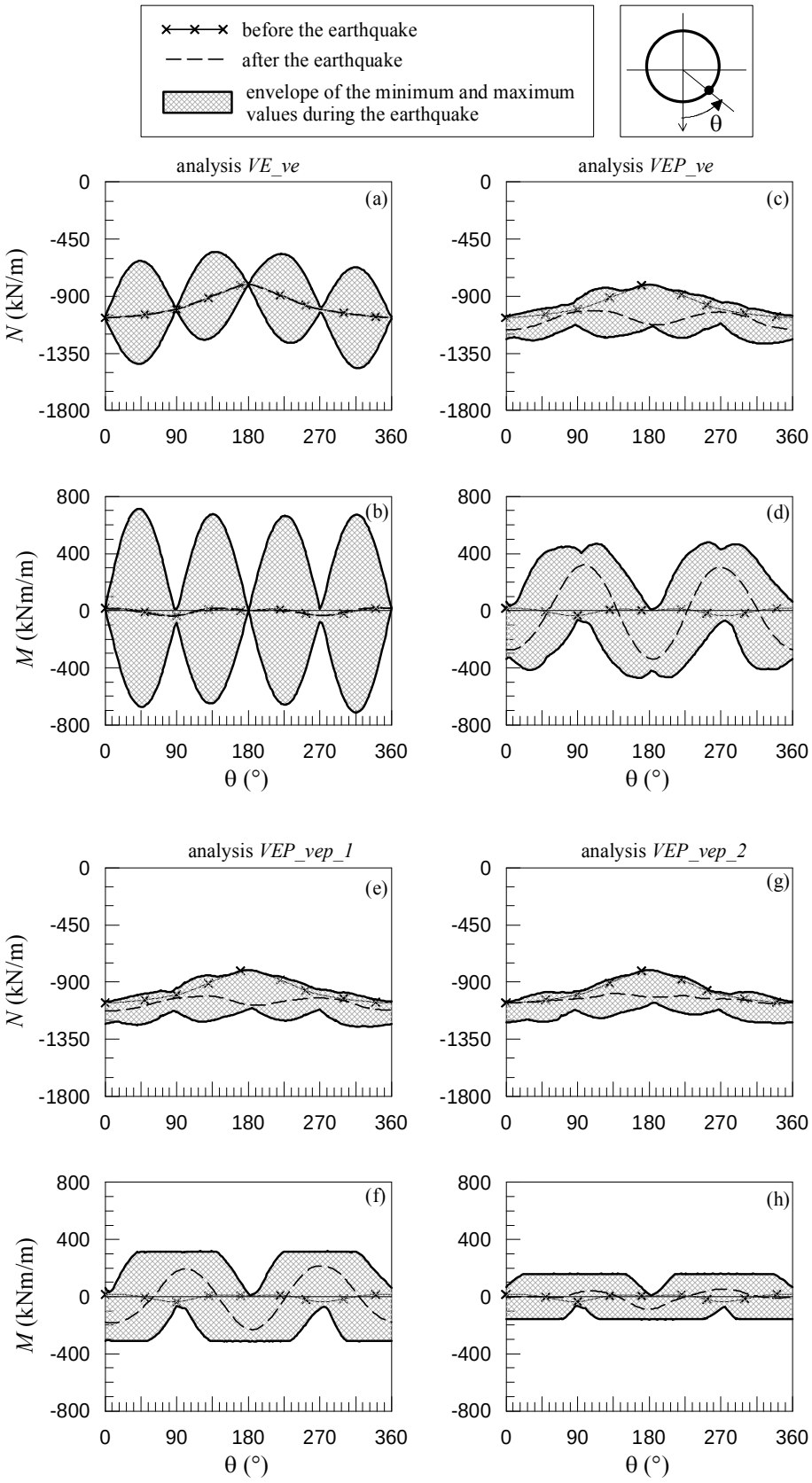

Fig. 10. Analyses VE_ve, VEP_ve, VEP_vep_1, VEP_vep_2: distribution of hoop force and bending moment before and after the seismic event and their maximum envelope.

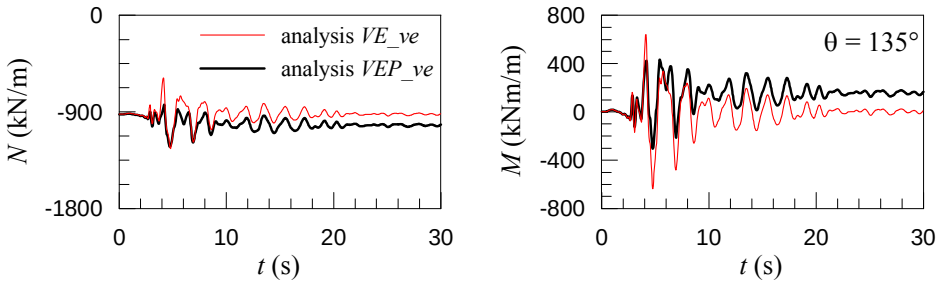

Fig. 11. Analyses VE_ve, VEP_ve: evolution of hoop force and bending moment during the earthquake ($0° \le \theta \le 135°$).

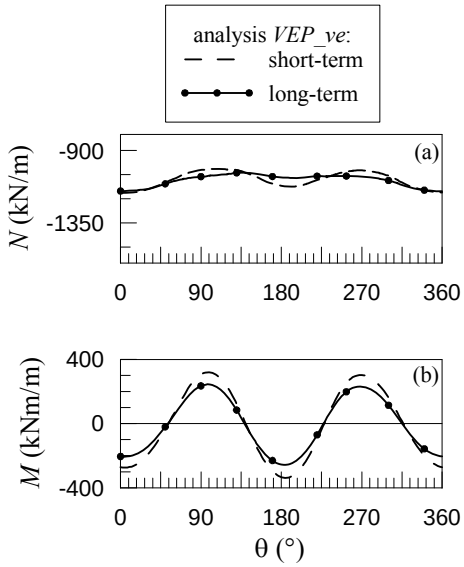

Fig. 12. Distribution of permanent hoop force and bending moment in the short- and long-term for the analysis VEP_ve.

results of the pushover analyses in terms of curvature of the lining: it results that in both cases the predicted maximum curvature (~0.007m^{-1} for *VEP_vep_1* and ~0.015m^{-1} for *VEP_vep_2*) is significantly lower than the ultimate one (0.16m^{-1} and 0.18m^{-1}, respectively), these latter being evaluated with reference to the constitutive model assumed for the tunnel section.

Regarding the performed pushover analyses, it is worth remarking that they provide more conservative results if compared to the corresponding dynamic ones. In fact, the absence of loading cycles leads to a significant increase in the number of lining sections in which the limit actions are reached.

Focusing only on the structural capacity, the obtained results highlight that a ductility-based design, capable of limiting the actions in the tunnel during and after the earthquake, would be particularly effective in reducing the cost of the structure.

Nonetheless, different conclusions can be drawn analysing the same results focusing on functionality issues. In fact, in the examined cases, even though the final rigid-body

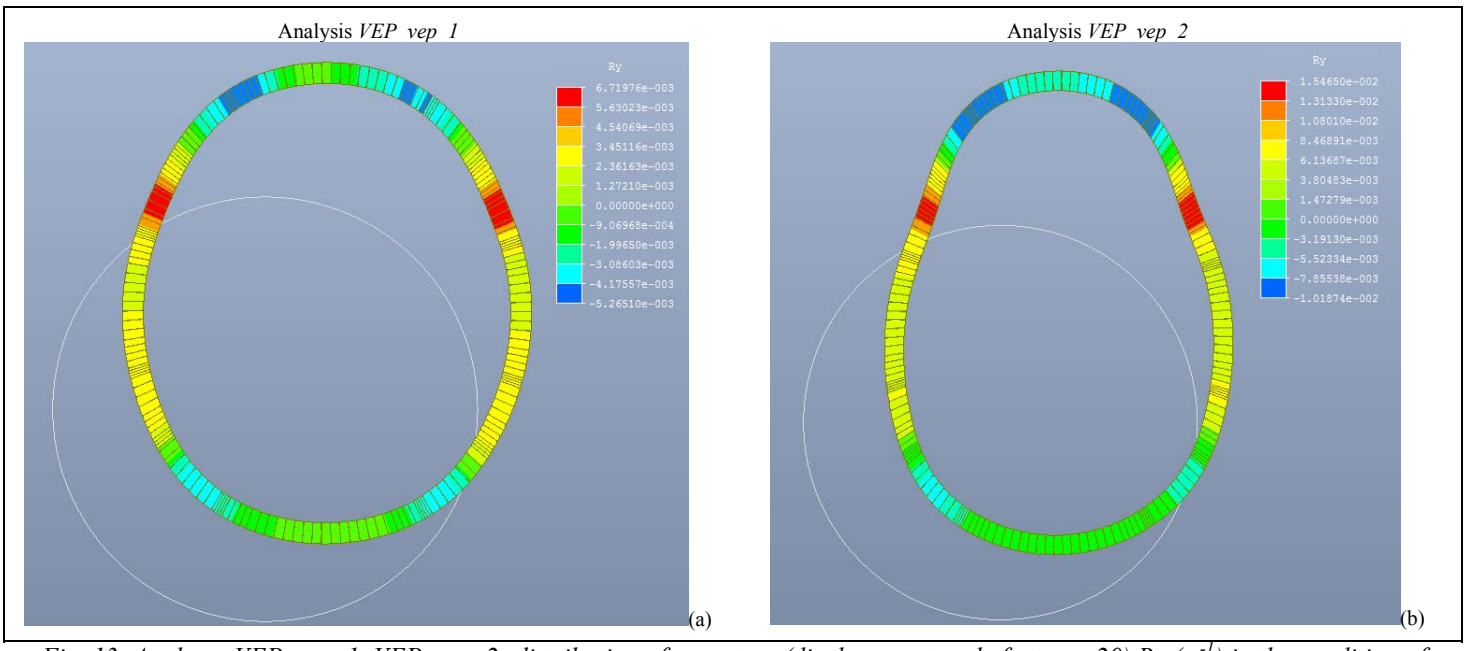

Fig. 13. Analyses VEP_vep_1, VEP_vep_2: distribution of curvature (displacement scale factor = 20) Ry (m^{-1}) in the condition of maximum deformation (t = 30 s).

displacements of the tunnel centre are very similar (0.141m in *VEP_ve*, 0.143m in *VEP_vep_1*, 0.149m in *VEP_vep_2*), the maximum final relative displacements between the tunnel and its centre are rather different (0.009m in *VEP_ve*, 0.025m in *VEP_vep_1*, 0.055m in *VEP_vep_2*). A larger curvature pattern implies a more widespread damage possibly leading to permanently opened cracks, affecting the durability of the tunnel.

This is the reason why, in the authors' opinion, it is not possible to define a-priori the appropriate ductility level for the design. Only a cost analysis, also including post-earthquake maintenance works, can provide indications on the optimized level of ductility capacity to be adopted.

Finally, the influence of structural cracking on the dynamic response was indirectly investigated by re-running in Plaxis and in Midas/Gen the *VEP_vep_1* analysis adopting a reduced stiffness for the lining (reduction factor equal to 0.5) to mimic the cracking related stiffness degradation. The distribution of the predicted hoop force N and bending moment M prior to and after the earthquake, as well as their minimum and maximum envelopes during the seismic event, are shown in Fig. 14a,b,c,d. No significant differences in terms of action envelope are evident when comparing the results. Figures 14b and 14d show a slight dissimilarity in terms of the final bending moment with an increase of the peak values in the analysis with reduced stiffness (M_{max} = 215 kNm/m and M_{min} = -231 kNm/m in *VEP_vep_ 1*; M_{max} = 252 kNm/m and M_{min} = -250 kNm/m in *VEP_vep_ 1* with reduced stiffness). Differently from the final actions, a general decrease in the predicted final deformation and displacements in the analysis with the reduced stiffness can be observed (Table 3 and Fig. 15).

CONCLUSIONS

This paper presents the results of a set of analyses aimed at studying the seismic transversal response of a shallow tunnel built in a soft clayey deposit. Two different approaches, both accessible in the engineering practice, are adopted to evaluate the increments of seismic-induced loads in the transverse direction of the tunnel lining in terms of hoop force and bending moment.

The first approach is the quasi-static one discussed in Wang (1993). It is based on a number of simplified hypotheses concerning the behaviour of the soil and the tunnel lining and their interaction, but has the advantage of generate straightforwardly reliable results without the need of employing sophisticated numerical procedures (Hashash *et al.* 2001).

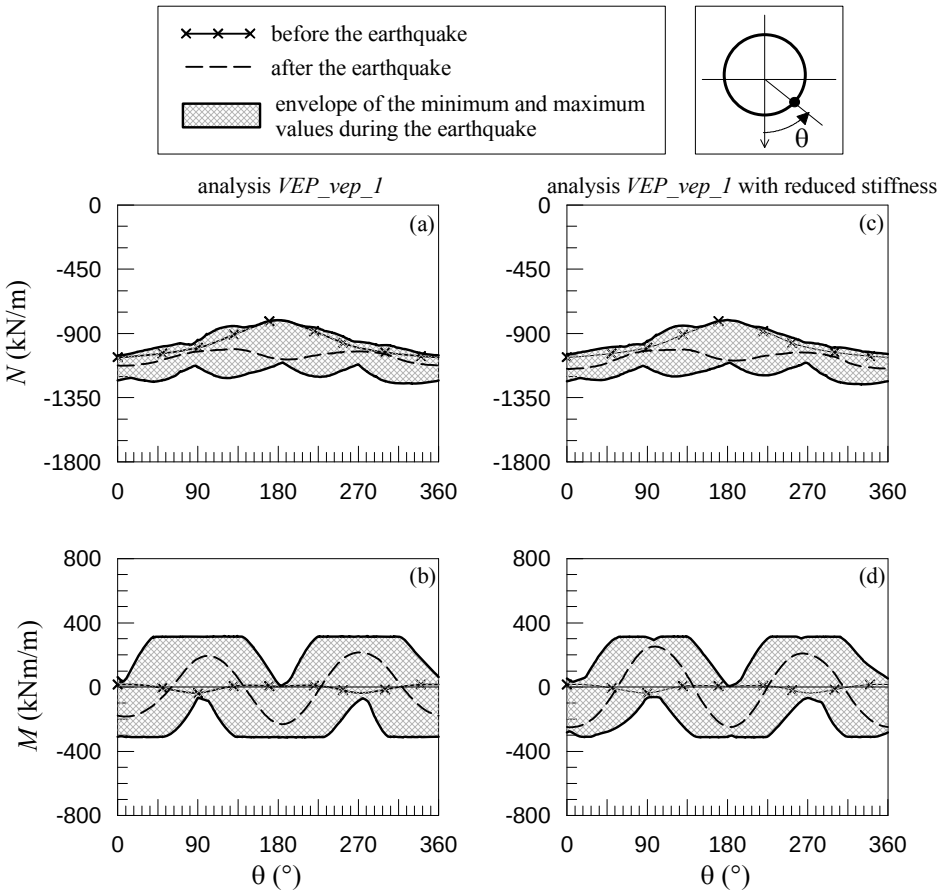

Fig. 14. Analyses VEP_vep_1, VEP_vep_1 with reduced stiffness: distribution of hoop force and bending moment before and after the seismic event and their maximum envelope.

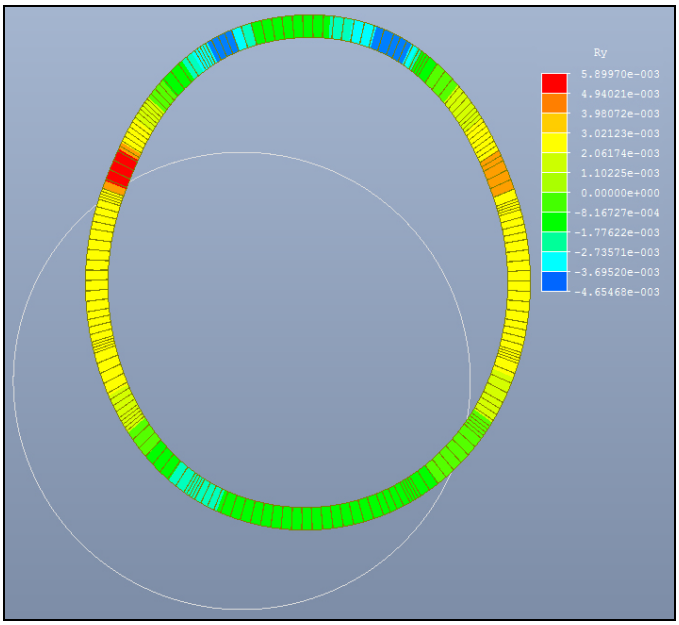

Fig. 15. Analyses VEP_vep_1 with reduced stiffness: distribution of final curvature (displacement scale factor = 20) Ry (m^{-1})

Table 3. Analyses *VEP_vep_1* and *VEP_vep_1* with reduced stiffness: main predicted values of the final deformation and displacement.

	VEP_vep_1	*VEP_vep_1* with reduced stiffness
Elongation of the horizontal diameter (m)	-0.044	-0.038
Elongation of the vertical diameter (m)	0.042	0.039
Maximum curvature (m^{-1})	$6.7 \cdot 10^{-3}$	$5.8 \cdot 10^{-3}$
Displacement of the tunnel centre (m)	0.143	0.138
Maximum final relative displacement between the tunnel and its centre (m)	0.025	0.022

The first approach is the quasi-static one discussed in Wang (1993). It is based on a number of simplified hypotheses concerning the behaviour of the soil and the tunnel lining and their interaction, but has the advantage of generate straightforwardly reliable results without the need of employing sophisticated numerical procedures (Hashash *et al.* 2001).

The second approach requires the execution of fully dynamic analyses using a non-linear Finite Element program, based on simple visco-elastic or visco-elasto-plastic constitutive assumptions.

The comparison between Wang's and FE visco-elastic solutions proved to be satisfactory: differences between the two approaches result to be about 10% both in terms of maximum increments in hoop force and bending moment acting in the lining.

FE results accounting for soil plasticity introduced new ingredients in the analysis of soil-tunnel interaction in dynamic conditions: different distribution and magnitude of the seismic-induced *N* and *M*, permanent increments of loads at the end of the seismic event and, eventually, further evolution of loads with time due to the post-seismic consolidation stage.

These features should be carefully considered in the design of underground structures in seismic areas.

Moreover, the FE analysis performed adding also a visco-elasto-plastic model for the tunnel indicated that, focusing only on the structural capacity of the system, a ductility-based design could be useful to reduce both the cost of the structure and the residual actions after the earthquake. If considering also functionality issues, a structural design based on a large ductility demand leads to a more widespread damage after the earthquake with an increase in the maintenance cost. This means that the identification of the 'optimum' ductility level of the structure should take into account not only its structural capacity but the overall cost, also including the potential maintenance works.

In the Author's opinion further research is needed in the direction of adopting more advanced constitutive models for both soil and tunnel lining, capable of reproducing more realistically their behaviour under dynamic conditions (e.g. Zienkiewicz *et al.* 1999).

REFERENCES

Amorosi, A. and D. Boldini [2009]. "Numerical modelling of the transverse dynamic behaviour of circular tunnels in clayey soils", *Soil Dyn. Earthquake Engrg*., No. 29(6), pp. 1059-1072.

Bardet, J.P., K., Ichii, and C.H. Lin [2000], "*EERA-A computer program for Equivalent-linear Earthquake site Response Analyses of layered soils deposits"*, User Manual.

Bathe, K.J. [1982]. "*Finite Element Procedures in Engineering Analysis"*, Prentice Hall, Upper Saddle River, New Jersey.

Biot, M.A. [1941]. "General theory of three-dimensional consolidation", *J. Appl. Phys*., No. 12, pp. 155-164.

CEN - European Committee for Standardization [2004a], "*EN 1992-1-1:2004 Eurocode 2. Part. 1-1 Design of concrete structures. General rules and rules for buildings*".

CEN - European Committee for Standardization [2004b], "*EN 1998-1:2004 Eurocode 8: Design of structures for earthquake resistance - Part 1: General rules, seismic actions and rules for buildings*".

Clough, R., and J. Penzien [2003]. "*Dynamics of Structures"*, Computers and Structures Inc..

Fardis, M.N., Carvalho, E., Elnashai, A., Faccioli, E., Pinto, P. and A. Plumier [2005]. "*Designers' Guide to EN 1998-1 and 1998-5. Eurocode 8: Design Provisions for Earthquake Resistant Structures"*, Thomas Telford Publishing.

Hashash, Y.M.A., Hook, J.J., Schmidt, B. and J.J. Yao [2001]. "Seismic design and analysis of under-ground structures", *Tunn. Undergr. Sp. Tech.,* No. 16, pp. 247-293.

Hashash, Y.M.A., Park, D. and J.I.C. Yao [2005]. "Ovaling deformations of circular tunnels under seismic loading, an update on seismic design and analysis of underground structures", *Tunn. Undergr. Sp. Tech*; No. 20, pp. 435-441.

Katona, M.C. and O.C. Zienkiewicz, O.C. [1985]. "A unified set of single step algorithms. III. The beta-m method, a generalization of the Newmark scheme", *Int. J. Numer. Methods Engrg.*, No. 21(7), pp. 1345-1359.

Kramer, S.L. [1996]. "*Geotechnical Earthquake Engineering"*, Prentice Hall, Upper Saddle River, New Jersey.

Lysmer, J. And R.L. Kuhlemeyer [1969]. "Finite dynamic model for infinite media", *ASCE EM*, No. 90, pp. 859-877.

MIDAS/Gen [2007]. "*Analysis Reference*", version 741.

PLAXIS [2003], "*Reference Manua*l", version 8.

Shahrour, I. and F. Khoshnoudian [2003], "Analysis of the seismic behavior of tunnels constructed in soft soils", *Proc. Int. Work. on Geotechnics of Soft Soils – Theory and Practice,* Noordwijkerhout, The Netherlands, pp. 339-344.

Viggiani, G.M.B. [1992], "*Small strain stiffness of fine grained soils"*, PhD thesis. City University. London.

Vucetic, M. and R. Dobry [1991]. "Effects of the soil plasticity on cyclic response", *Journal of Geotech. Eng. Div., ASCE,* No. 117(1), pp. 89-107.

Wang, J.N. [1993]. "*Seismic design of tunnels: a state-of-the-art approach"*, Monograph 7, Parsons, Brinckerhoff, Quade & Diuglas Inc., New York.

Woodward, P.K. and D.V. Griffiths [1996]. "Influence of viscous damping in the dynamic analysis of an earth dam using simple constitutive models", *Comput. Geotech.*, No. 19(3), pp. 245-263.

Zienkiewicz, O.C., Chan, A.H.C., Pastor, M., Schrefler, B.A. and T. Schiomi [1999]. "*Computational Geomechanics with Special Reference to Earthquake Engineering"*, John Wiley & Sons, Chichester, UK.